ORIGINAL ARTICLE

Testing and validating IRI-2016 model over Ethiopian ionosphere

Lake Endeshaw[1]

Abstract This paper focuses on the validation of the latest version of the International Reference Ionosphere (IRI-2016) model in predicting the vertical total electron content (VTEC) variation over Ethiopian ionospheric region during a high solar activity (2012-2016) phase. The diurnal, monthly and seasonal VTEC variations were analyzed from dual-frequency global positioning system (GPS) and IRI-2016 model at the Debark station. The diurnal, monthly and seasonal maximum TEC values measured between around 9:00 and 18:00 UT (12:00 and 21:00 LT) hours and the minimum TEC values measured before 9:00 (12:00 LT) and after 18:00 UT (21:00 LT). The overall results show that IRI-2016 model generally overestimates the diurnal, monthly and seasonal mean VTEC values during the high solar activity (2012-2016) phase. The model prediction generally follows that the monthly and seasonal variations of the measured VTEC values in equinoctial months are higher than solstice months. The monthly mean and seasonal mean values of IRI-TEC and GPS-TEC mostly correlates before early morning and after evening hours and also slightly IRI-TEC underestimates starting from morning hours up to evening hours. The magnetic storm effects on GPS-TEC are associated with fluctuations. However, the IRI-TEC values show smooth pattern during both in storm on and off options. Consequently, the IRI-2016 model does not correctly respond to the effects of the resulting storm disturbance.

Keywords GPS-VTEC · IRI-2016 VTEC · VTEC

✉ L. Endeshaw
endeshawlake@gmail.com

[1] Department of Physics, Worabe University, Worabe, Ethiopia

1 Introduction

The large natural blanket of plasma in the atmosphere, which envelopes the Earth from an altitude of approximately 50 km to several thousands of kilometers is called the ionosphere. The existence of the ionosphere was clearly established in 1901 when G. Marconi successfully transmitted radio signals across the Atlantic (Ratcliffe 1967). The free electrons and ions are produced via ionization of the neutral particles both by extreme ultraviolet radiation from the Sun and by collisions with energetic particles that penetrate the atmosphere (Newell 1980). The ionized particles in the ionosphere are produced during the daytime through absorption of solar extreme ultraviolet and x-ray radiation by the atmospheric species. As the ionizing radiation from the sun penetrates deeper and deeper into the Earth's atmosphere, it encounters a larger and larger density of gas particles, producing more and more electrons per unit volume (Bittencourt 2004). The recombination of free electrons with positive ions is a reversion of the photoionization and the recombination process is the main driver to produce neutral atoms (Limberger et al. 2015).

Diurnal ionospheric variation is the change in ionospheric electron concentration from day to night brought about by the daily rotation of the Earth (Liu and Chen 2009). During the day when the Sun is directly overhead, the intensity of sunlight reaching the upper atmosphere is greatest and the level of ionization is maximized. At night side of the Earth, the amount of sunlight reaching the atmosphere is zero and production due to photoionization is reduced to the lowest level. The diurnal variation of the ionosphere is generally controlled by the photoionization, recombination and transport processes (Wernik et al. 2004). Ionospheric seasonal variation is related to a solar zenith angle change, while its solar cycle variation is related to a change in the solar EUV and X-ray radiation fluxes. Solar cycle is associated

with the Sun spot numbers and Sun spot is the coldest part of sun. The Sun's output of energy is not constant in time but changes over a period of 11 years cycle, which is measured in terms of the number of sunspot visible on the disk (Hunsucker and Hargreaves 2002). Variations linked to solar activity are associated with solar EUV radiation and X-ray flux, and geomagnetic activity are associated with the solar wind-magnetosphere ionosphere coupling (Athieno 2017).

Geomagnetic storms and associated ionospheric storms occur when charged particles with high energy in the solar wind, arrive to the Earth causing interferences in the terrestrial magnetic field. The charged particles interacting with the atmosphere excite ions and produce additional electrons. The equatorial regions like Ethiopia can be characterized with combined effect of high radiation level from the sun and the electric and the magnetic fields of the Earth results in the electrons rising. And moving along the horizontal lines of the magnetic field and makes a particle to transport and penetration of high-latitude electric field to lower latitude which travel equator ward with high velocities during the storm.

At present most models are able to reproduce consistently the climate of the ionosphere over a given location or region, as defined mostly by diurnal, seasonal and solar cycle variations (Abdus Salam Intern 2009). In the late 1970's the first International Reference Ionosphere model (IRI) was released with Rawer as its first Chairperson (Rawer et al. 1978). The IRI Working Group of International Ionospheric experts are developing the model as new data become available and order data sources are fully evaluated and exploited, the model should be revised in accordance with these new results. Many researchers have made different studies on IRI-TEC and GPS-TEC over different regions of the world and the IRI model has been steadily improved as IRI-78 (Rawer et al. 1978), IRI-85 (Bilitza 1986), IRI-1990 (Bilitza 1990), IRI-2000 (Bilitza 2001), IRI-2007 (Bilitza and Reinisch 2008), IRI-2012 (Bilitza et al. 2014) and the latest is IRI-2016 (Bilitza et al. 2017).

Ezquer et al. (1998) has shown that the IRI-95 model TEC generally overestimates the observed TEC during the daily minimum and underestimates it in the remaining hours of the day. The IRI-2000 model overestimates the measurement in low-latitude (Bhuyan and Borah 2007). The IRI-2001 has the discrepancies between the experimental and model TEC values during high solar activity years (Mukherjee et al. 2010). The studies have been made to evaluate the performance of the IRI model in the East African regions during low solar activity yeas (2009-2011) over Kenya regions (Olwendo et al. 2012a) have studied that seasonal average of ETC estimated from the IRI-2007 model are significantly higher than GPS measurements, which is in agreement to this study. Additionally, for solar activity phase 2009-2010 (Olwendo et al. 2012b) also studied the IRI-2007

model overestimates for all the seasons only except during the March equinox. Tariku (2015) studied the discrepancy in the IRI-2012 model performance using IRI-NeQ topside option over equatorial regions of Ethiopia during low solar activity year 2009 and high solar activity year 2012. His results showed that the diurnal VTEC prediction performance of the model is generally better during the solar minimum phase 2009 than during solar maximum phase 2012 which is in agreement to this study (Tariku et al. 2014). Kumar (2016) studied IRI-2012 model with respect to ground based GPS measurements during ascending phase of solar activity in 2009 to 2013 from low to mid-latitudes and they found that low-latitude regions higher than mid-latitude discrepancies during all the seasons (Kumar et al. 2015).

In this paper, I have studied the variations of the GPS-TEC and IRI-2016 model during high solar activity phase from 2012 to 2016. Hence, this is perhaps the first work to extensively assess the VTEC variation and examine the capacity of the latest version (IRI-2016) model in predicting the VTEC during high solar activity phase. As a result, in this study a very high (2012-2016) solar activity phase considered to see the diurnal, monthly and seasonal VTEC variations and capability of IRI-2016 model over Ethiopian regions.

2 Methods

The observation data from GPS-TEC and IRI-TEC data were collected from March 2012 to December 2016 from Ethiopia at *Debark station* (*geographic* 13.15° N, 37.89° E; *geomagnetic* 9.52° N, 112.84° E). The description of these two data sets is discussed in the following Sects. 2.1 and 2.2.

2.1 TEC from the International Reference Ionosphere (IRI-2016) model

The IRI is an international project sponsored by the Committee on Space Research (COSPAR) and the International Union of Radio Science (URSI). The TEC from IRI-2016 model can be calculated according to IRI 2016 home page.[1] In this work the year is chosen from 2012 to 2016 and their months and days of each year are imported. Local time in Ethiopia is 3 hours a head of Universal Time (i.e., LT = UT + 3 hours).

2.2 TEC from dual-frequency GPS receiver

The ionospheric parameter that has an over bearing influence on the GPS based communication and navigation systems is the total electron content (TEC) (Akala et al. 2013).

The GPS measurements are used to estimate the TEC along a ray path between a GPS satellite and receiver on the ground. These GPS measurements are recorded by dual-frequency GPS receivers as they are better to eliminate ionospheric errors in the estimation of TEC. GPS have dual frequencies f_1 and f_2, which are derived from the fundamental frequency f_o (Gao and Liu 2002). A dual-frequency GPS receiver can measure the difference in ionospheric delays between the L1 and L2 of the GPS frequencies, which are generally assumed to travel along the same path through the ionosphere. GPS observables are either code pseudo ranges (P) or carrier phase (Φ) measurements (Klobuchar et al. 1996).

$$f_o = 10.23 \text{ MHz} \tag{1}$$

$$f_1 = 154 f_o = 1575.42 \text{ MHz} \tag{2}$$

$$f_2 = 120 f_o = 1227.60 \text{ MHz} \tag{3}$$

Thus, the group delay can be obtained as:

$$P_1 - P_2 = 40.3 \text{ TEC} \left\{ \frac{1}{f_2^2} - \frac{1}{f_1^2} \right\} \tag{4}$$

$$\text{TEC}_P = \frac{1}{40.3} \frac{f_1^2 f_2^2}{f_1^2 - f_2^2} \{ (P_2 - P_1) \} \tag{5}$$

where, p_1 and p_2 are the group path lengths corresponding to the frequency of the high GPS ($f_1 = 1575.42$ MHz) and the frequency of the low GPS ($f_2 = 1227.61$ MHz) respectively.

Conversely, the TEC from carrier phase measurements can be expressed as:

$$\text{TEC}_\Phi = \frac{1}{40.3} \frac{f_1^2 f_2^2}{f_1^2 - f_2^2} \{ (\varphi_1 - \varphi_2) \} \tag{6}$$

where, $(\varphi_1 - \varphi_2)$ is the phase measurements and they are obtained from the fundamental frequency (Klobuchar et al. 1996; Ciraolo et al. 2007).

TEC can also be calculated by integrating with location dependent ds electron density ne(s). The TEC is the amount of free electrons along the path of the electromagnetic wave between each satellite and the receiver, given by

$$\text{TEC} = \int_{\text{receiver}}^{\text{satellite}} \text{ne}(s)\, ds \tag{7}$$

The GPS-TEC data utilized for this work are inferred from the dual-frequency GPS installed at Ethiopia in Debark station (Geographic latitude 13.2° N and longitude 37.9° E; Geomagnetic latitude 9.52° N and longitude 112.48° E). My implementation in averaging the GPS-TEC and IRI-TEC in studying the diurnal, monthly and seasonal climatology is 15-minute resolution. All data scripts were written for this work to import, process and plot for GPS and model output by Matrix Lab software (MATLAB) version 2016b.

3 Results

3.1 Diurnal variation of VTEC and validation of IRI-2016 model

Diurnal variation of TEC is measured with different amount of total electron content between day, night and hourly TEC variation in 24 hours of a day. I have plotted about 57 diurnal variation of VTEC and validation of IRI-2016 model plots in between March 2012 to December 2016 and those plots are grouped in to three fits, which are best fit, intermediate fit and worst fit based on the performance of the IRI-2016 model estimates to detect TEC variation. I have selected the particular months among those plots, which are categorized under best fits, intermediate fits and worst fits of IRI-2016 model estimate.

The first figure is best fit (Fig. 1); the next figure is intermediate fit (Fig. 2) and also the last figure (Fig. 3) is worst fit of IRI-2016 model estimate. In Fig. 1, September 2013 indicates that a good agreement with slightly less overestimate or underestimate in the observation and IRI-2016 model estimate. In October 2012 (partially in most hours and days of the month) indicates that slightly a good agreement (intermediate fits) as shown in Fig. 2. May 2015 shows only about 3 to 31 days in the first 5:00 UT hours and the last days of the month in the last hours of the day slightly a good agreement, but overestimates at between 6:00 UT to 18:00 UT hours in all most all days of the month and underestimating from 0:00 UT to 3:00 UT hours at the 6, 9, 10, 11 and 12 days.

3.2 Storm time VTEC variation and validation of IRI-2016 model

The response of the ionosphere to geomagnetic activity commonly called ionospheric storms (Mendillo 2006). There are about 34 storm days during high solar activity phase from 2012 to 2016 years. The sample storm days used in this paper for statistical treatment of the VTEC variation and performance of the IRI-2016 model are 12 storm events. The IRI-2016 storm model had been switched on and the storm time effect on the measured and modeled VTEC values were observed by considering a magnetic storm day with a Dst index of minimum (-50 nT) occurred in the five years of the months to capture VTEC values and variations (Gonzalez et al. 1994; Prolss 2004; Gopalswamy et al. 2007).

As shown in Fig. 4, GPS-VTEC values show fluctuations during storm days; but the IRI-2016 model VTEC values do not show notable fluctuations in all the five year

Fig. 1 Diurnal TEC variation and validation of IRI-2016 model and GPS observations in September 2013 (best fit)
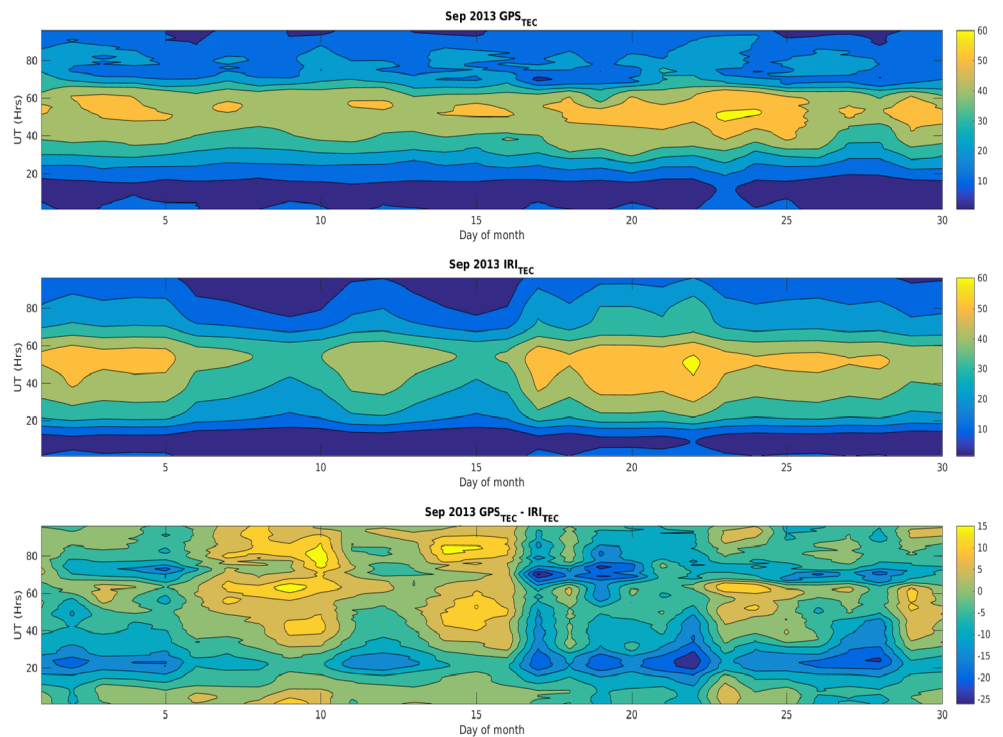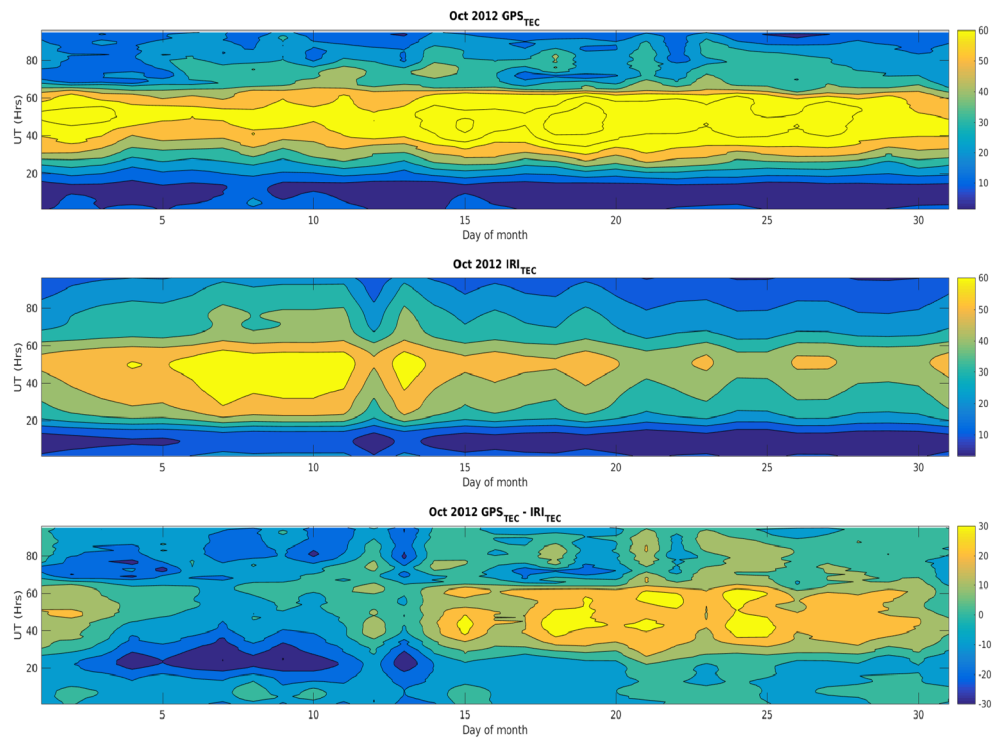

Fig. 2 Diurnal TEC variation and validation of IRI-2016 model and GPS observations in October 2012 (intermediate fit)

month days in storm on options (Tariku 2015). As shown in the Fig. 4 and Table 1, the pattern of the mean between the IRI-TEC values in the storm on and storm off options have slightly the same values of TECU (37.38, 26.28, 45.26, 30.12, 26.78 TECU) and (37.67, 26.35, 45.67, 30.3, 26.85 TECU) respectively; which is slightly different from GPS-

TEC valves (32.8, 18.8, 40.27, 37.46 and 27.24 TECU) in five year selected storm time months. Consequently, the IRI-2016 model does not correctly respond to the effects of the resulting storm disturbance. Moreover, the GPS-TEC values show fluctuations by responding to the effects of the resulting storm disturbance.

Fig. 3 Diurnal TEC variation
and validation of IRI-2016
model and GPS observations in
May 2015 (worst fit)
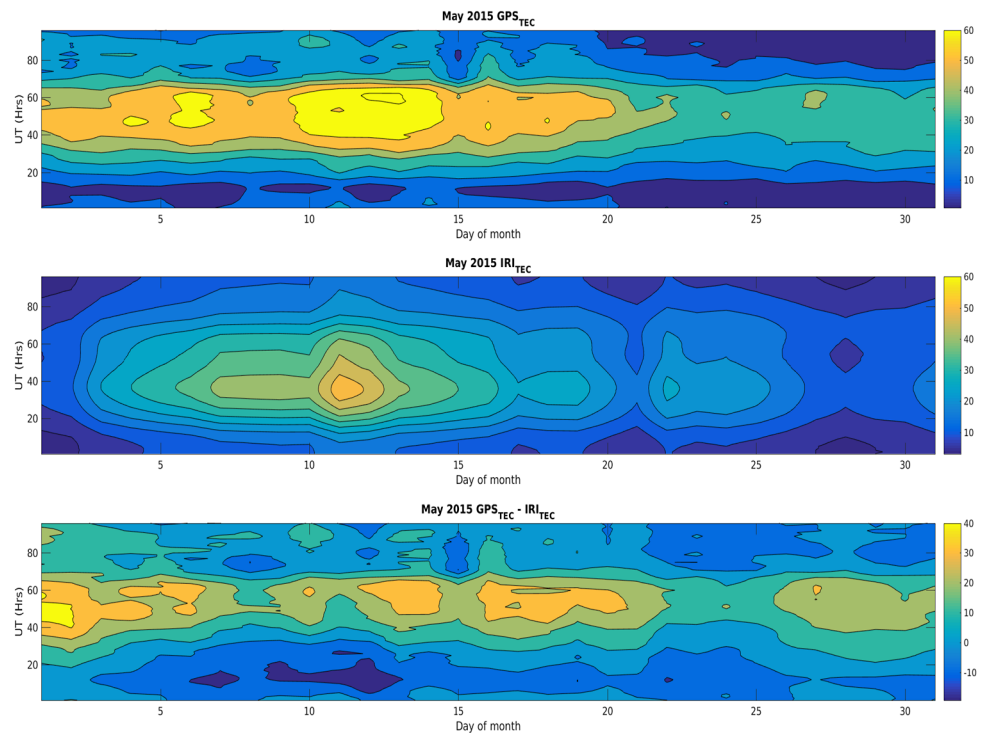
3.3 Monthly variation of VTEC and validation of IRI-2016 model

In Fig. 5, the monthly mean of IRI-TEC and GPS-TEC correlates at 2:00, 8:00 and 17:00 UT in March; at 9:00 and 16:00 UT hours in November; at around 2:00, 7:00, and above 16:00 UT in October. The model underestimates from 8:00 to 17:00 UT in (March, October and November) and overestimates totally in May. In Fig. 6, the monthly mean of IRI-TEC and GPS-TEC correlates at 2:00, 8:00 and 17:00 UT in February, at most hours in September; but the model underestimates from 8:00 to 17:00 UT in (February and September) and overestimates totally in (January and June) and partially in other months.

In Fig. 7, the monthly mean of IRI-TEC and GPS-TEC correlates from 8:00 to 15:00 UT in April, at 8:00 and 17:00 UT hours in December; but the model underestimates from 8:00 to 17:00 UT in December and overestimates totally in (July and August) and partially in other months of the year 2014. In Fig. 8 the monthly mean of IRI-TEC and GPS-TEC correlates at 2:00, 8:00 and 17:00 UT in January, from 0:00 to 2:00, 7:00 UT in March, from 15:00 to 17:00 UT in September, at around 2:00, 9:00, 16:00 UT in November, but the model underestimates from 8:00 to 17:00 UT in November, above 7:00 UT in March and overestimates totally in (July and November). The monthly mean of IRI-TEC and GPS-TEC correlates from 0:00 to 2:00 UT, 15:00 to 16:00 UT, 23:00 to 24:00 UT in April, at 2:00 UT in December and overestimates totally in (May, August and December) and mostly in other months of the year 2016 (Fig. 9).

3.4 Seasonal variation of VTEC and validation of IRI-2016 model

In Fig. 10, the seasonal mean of IRI-TEC and GPS-TEC correlates in at 8:00 UT, 16:00 UT in 2012 March equinox, from 1:00 UT to 2:00 UT, at 8:00 UT, at 17:00 UT and from 21:00 to 22:00 UT hours in 2012 September equinox and at 8:00 and 16:00 UT hours in 2012 December solstice. But the model underestimates slightly from 8:00 to 16:00 UT hours in 2012 March equinox, 2012 September equinox and 2012 December solstice and overestimates totally in 2012 June solstice, from 0:00 to 8:00 UT and above 16:00 UT hours in 2012 March equinox, 2012 September equinox and 2012 December solstice seasons of the year 2012. In Fig. 11, the seasonal mean of IRI-TEC and GPS-TEC correlates in slightly from 9:00 to 16:00 UT in 2013 March equinox, from 14:00 UT to 16:00 UT hours in 2013 September equinox and at 10:00 and 16:00 UT hours in 2013 December solstice. But the model underestimates slightly from 8:00 to 13:00 UT hours in 2013 December solstice and overestimates totally in 2013 June solstice and 2013 September equinox; from 0:00 to 9:00 UT and above 15:00 UT hours in 2013 March equinox and 2013 December solstice seasons of the year 2013 in Fig. 11. In Fig. 12, seasonal mean of IRI-TEC and GPS-TEC correlates in from 9:00 to 15:00 UT in 2014 March equinox, at 10:00 UT and 16:00 UT hours in 2014 September equinox and at 8:00 and 16:00 UT hours in 2014 December solstice. The model underestimates slightly from 8:00 to 13:00 UT hours in 2014 March equinox, from 9:00

Fig. 4 The storm time VTEC
variation and validation of
IRI-2016 model and GPS
observation values when the
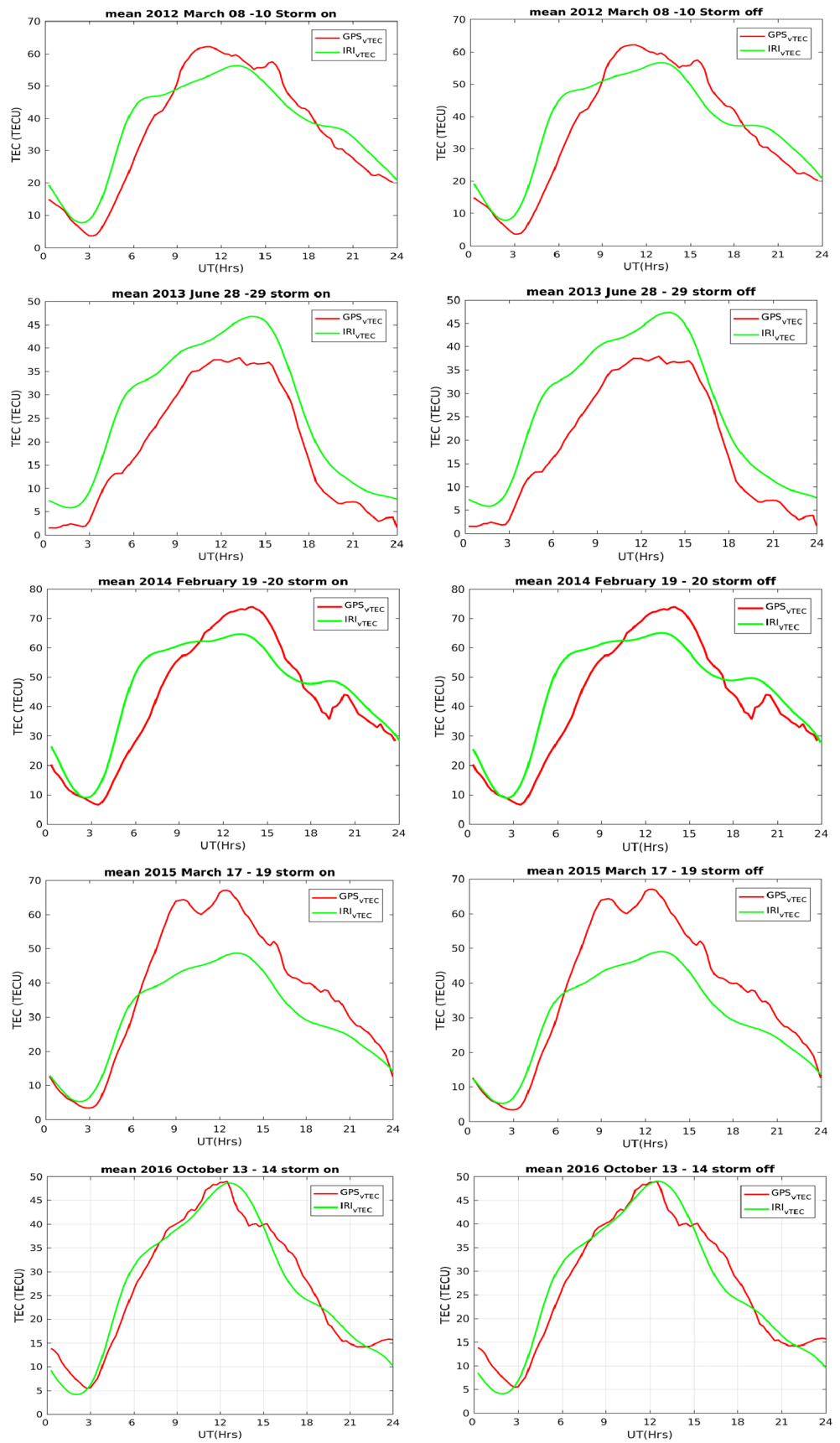storm option is on and off
between 2012-2016 years

Table 1 IRI-2016 Model IRI_TEC value in storm "on" and "off" and storm disturbance GPS_TEC observation values

Year	IRI_TEC(TECU)						GPS_TEC(TECU)		
Selected storm times (2012-2016)	Storm on			Storm off			Min	Max	Mean
	Min	Max	Mean	Min	Max	Mean			
March 08–10 2012	7.67	56.23	37.38	7.933	56.6	37.67	3.554	62.05	32.8
June 28–29 2013	5.8	46.7	26.28	5.8	47.3	26.35	1.519	37.94	18.8
February 19–20 2014	9	64.7	45.26	8.85	65.1	45.69	6.537	74.01	40.27
March 17–19 2015	5.333	48.6	30.12	5.267	48.97	30.32	3.393	67.01	37.46
October 13–14 2016	4.1	48.7	26.78	4.05	49.1	26.85	5.446	49.04	27.24

Fig. 5 Monthly TEC variation and validation of IRI-2016 model and GPS observations in 2012 months
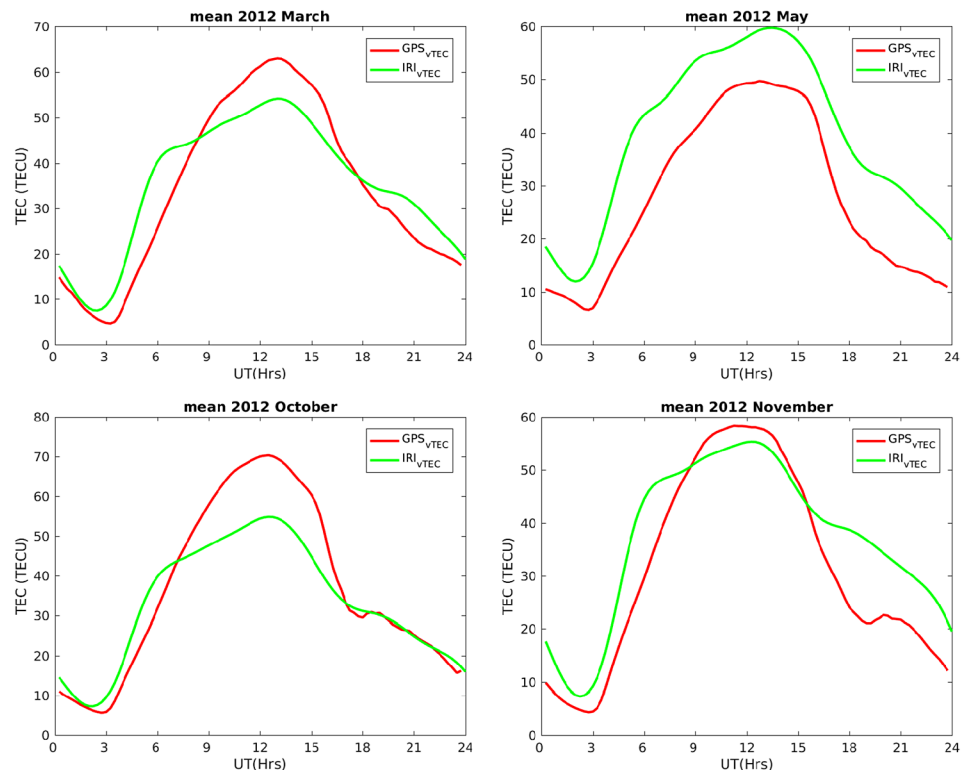
to 16:00 UT hours in 2014 September equinox and 2014 December solstice. And the model overestimates totally in 2014 June solstice, from 0:00 to 9:00 UT and above 15:00 UT hours in 2014 March equinox, 2014 September equinox and 2014 December solstice seasons.

In Fig. 13, seasonal mean of IRI-TEC and GPS-TEC correlates in from 0:00 to 2:00 UT, at 7:00 UT in 2015 March equinox, from 16:00 to 17:00 UT hours in 2015 September equinox, at 8:00 UT and above 18:00 UT in 2015 June solstice and at 2:00, 8:00 and 17:00 UT hours in 2015 December solstice. The model underestimates at above 7:00 UT hours in 2015 March equinox, from 8:00 to 18:00 UT hours in 2015 June solstice and 2015 December solstice. In addition, the model overestimates totally in 2015 September equinox, from 2:00 to 7:00 UT hours in 2015 March equinox, from 0:00 to 8:00 UT hours in 2015 June solstice

and from 0:00 to 8:00 UT and above 18:00 UT hours in 2015 December solstice seasons of the year 2015 in Fig. 13. The seasonal mean hourly modeled VTEC values and the measured GPS VTEC are mostly correlated in 2016 March equinox and for the others in the first 3:00 UT hours and above the 15:00 UT hours. The seasonal mean hourly modeled VTEC values are found to be larger than the corresponding measured VTEC values in all seasons during both in equinox and solstice of the year 2016. In general, the modeled VTEC value overestimates for all the seasons in the years 2012 to 2016.

4 Discussions

In the magnetic storm days GPS-VTEC observation values show fluctuations (many up and down peaks), but the IRI-

Fig. 6 Monthly TEC variation and validation of IRI-2016 model and GPS observations in 2013 months
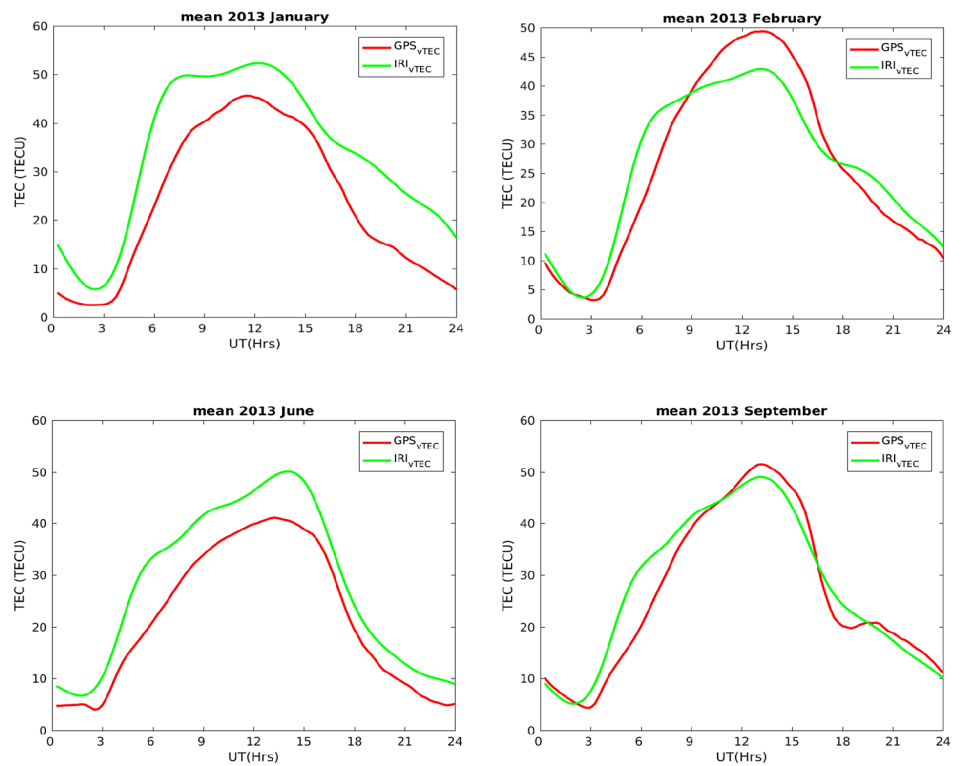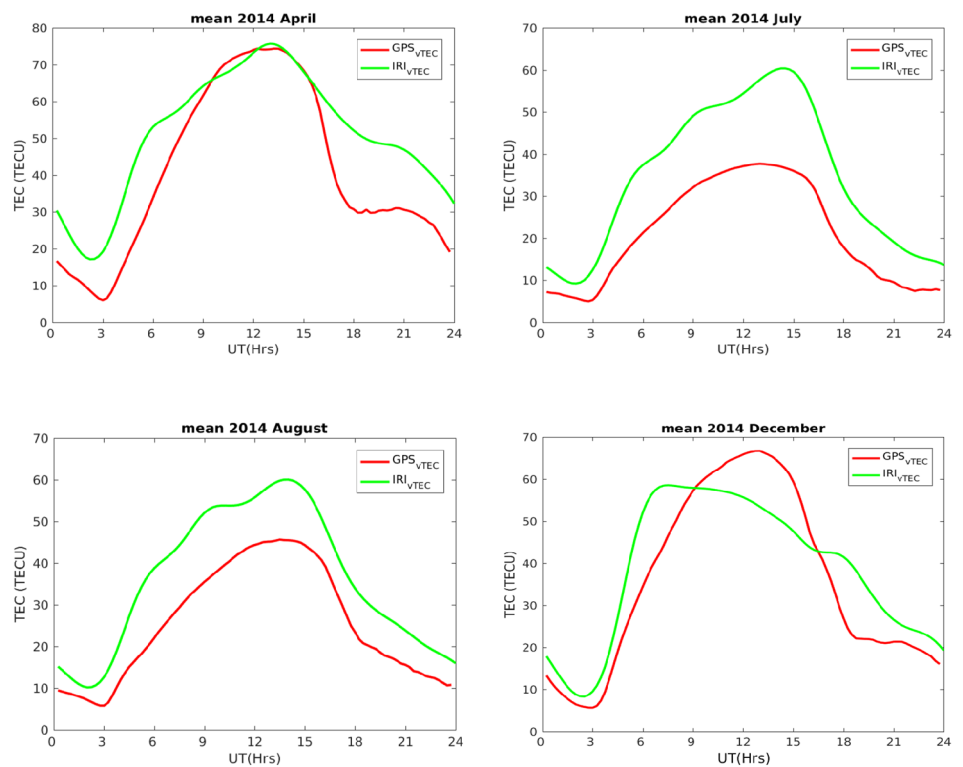

Fig. 7 Monthly TEC variation and validation of IRI-2016 model and GPS observations in 2014 months

2016 model VTEC values do not show notable fluctuations in all the five year month days during in both storm on and off options (see Fig. 4 and Table 1). Consequently, the IRI-2016 model does not correctly respond to the effects of the resulting storm disturbances. The monthly mean VTEC values attained their minimum value in between 00:00 UT and 3:00 UT (3:00 LT and 6:00 LT) and increases steeply up to about 12:00 UT (15:00 LT) with peak value and gradu-

Fig. 8 Monthly TEC variation and validation of IRI-2016 model and GPS observations in 2015 months
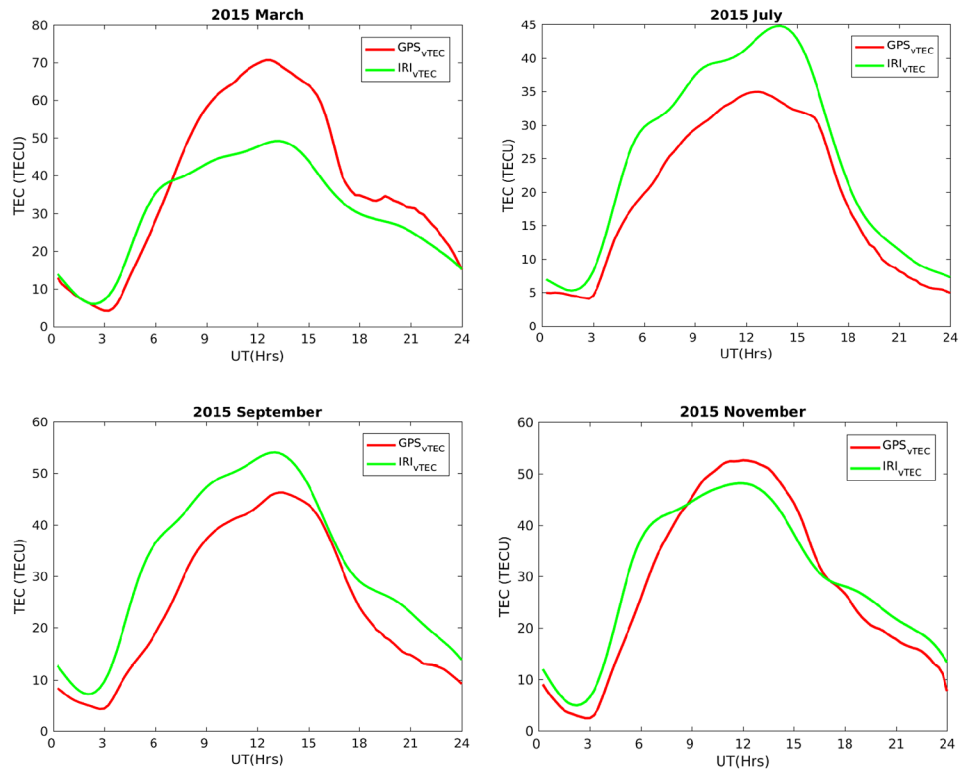
Fig. 9 Monthly TEC variation and validation of IRI-2016 model and GPS observations in 2016 months
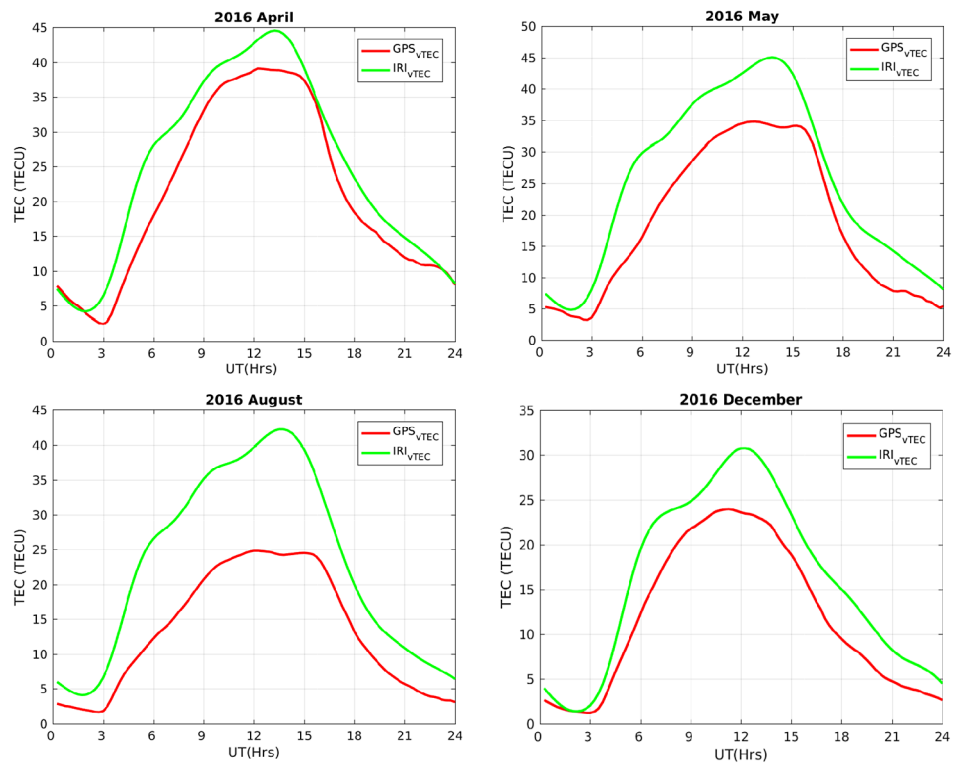
ally declines up to 21:00 UT (0:00 LT) and after this VTEC value attained its minimum value again. The seasonal VTEC value attained their peak values about 12:00 UT (15:00 LT) to 15:00 UT/18:00 LT hours and attained minimum val-

ues in 0:00 UT-3:00 UT (3:00 LT-6:00 LT) and 21:00-0:00 UT (0:00-3:00 LT). The seasonal observed discrepancies between the GPS-VTEC and modeled VTEC values have been slightly occurred in the time interval between 9:00 and

Fig. 10 Seasonal TEC variation and validation of IRI-2016 model and GPS observations in 2012 seasons
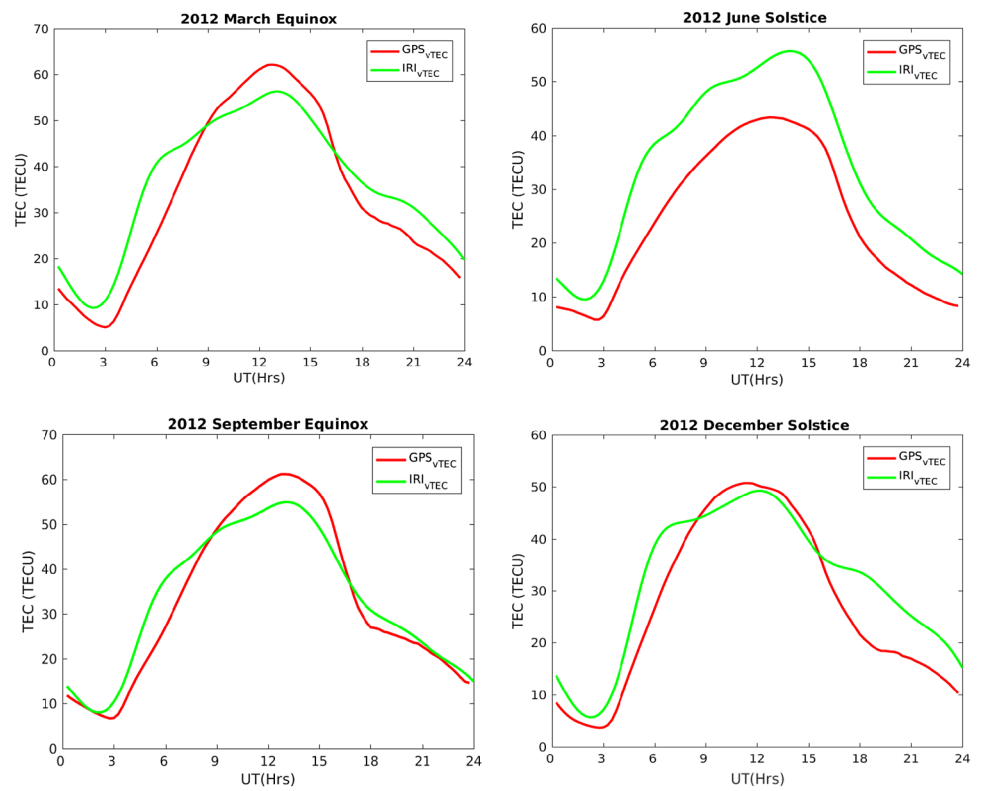
Fig. 11 Seasonal TEC variation and validation of IRI-2016 model and GPS observations in 2013 seasons
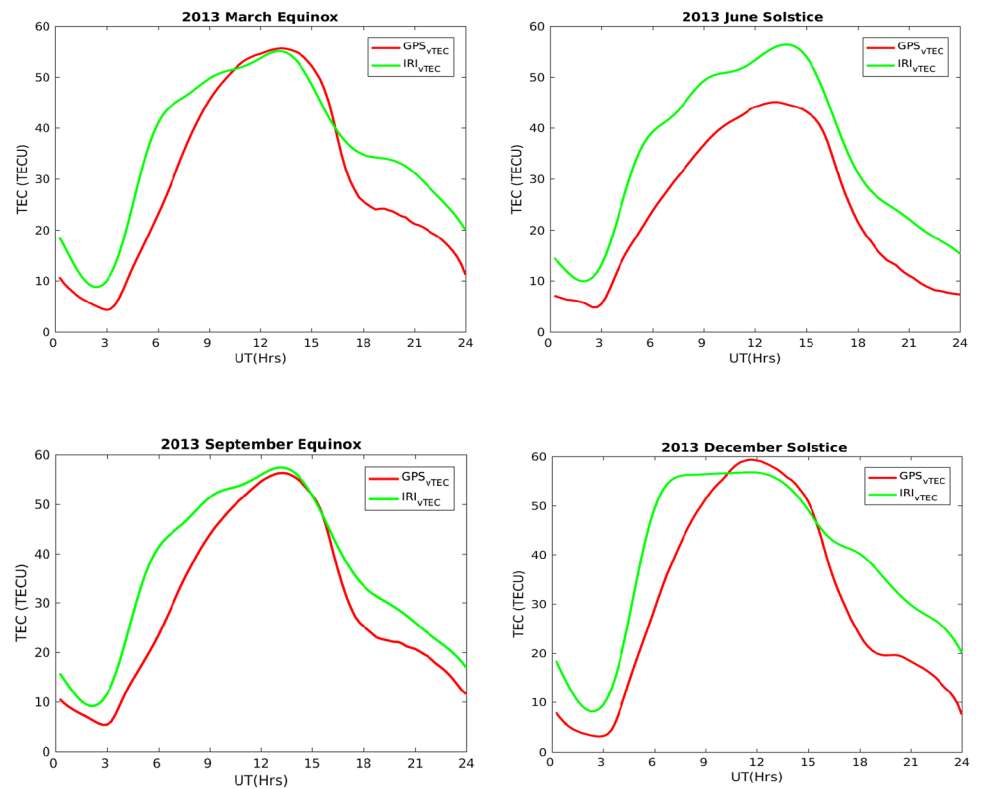
15:00 UT (12:00-18:00 LT), which is similarly as noted by different findings (Rios et al. 2007; Nigussie et al. 2013; Oyekola 2012; Sethi et al. 2011).

The model prediction generally follows that the monthly and seasonal variations of measured VTEC in equinoctial monthly values is higher than in solstice months. The de-

Fig. 12 Seasonal TEC variation and validation of IRI-2016 model and GPS observations in 2014 seasons
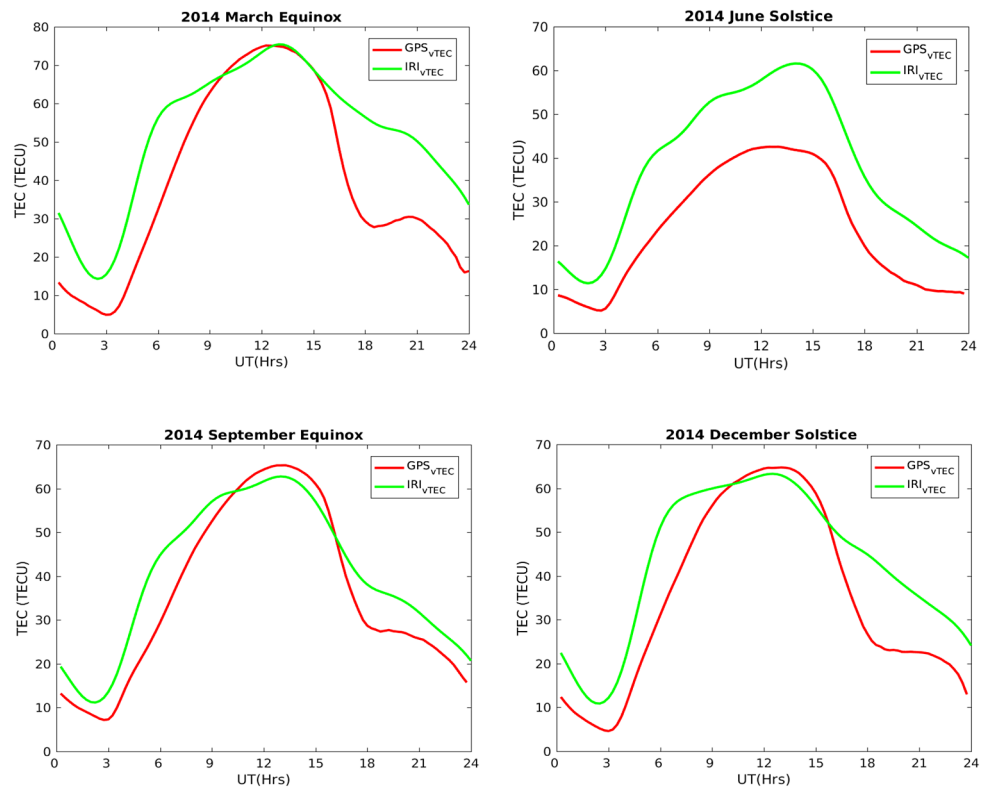

Fig. 13 Seasonal TEC variation and validation of IRI-2016 model and GPS observations in 2015 seasons
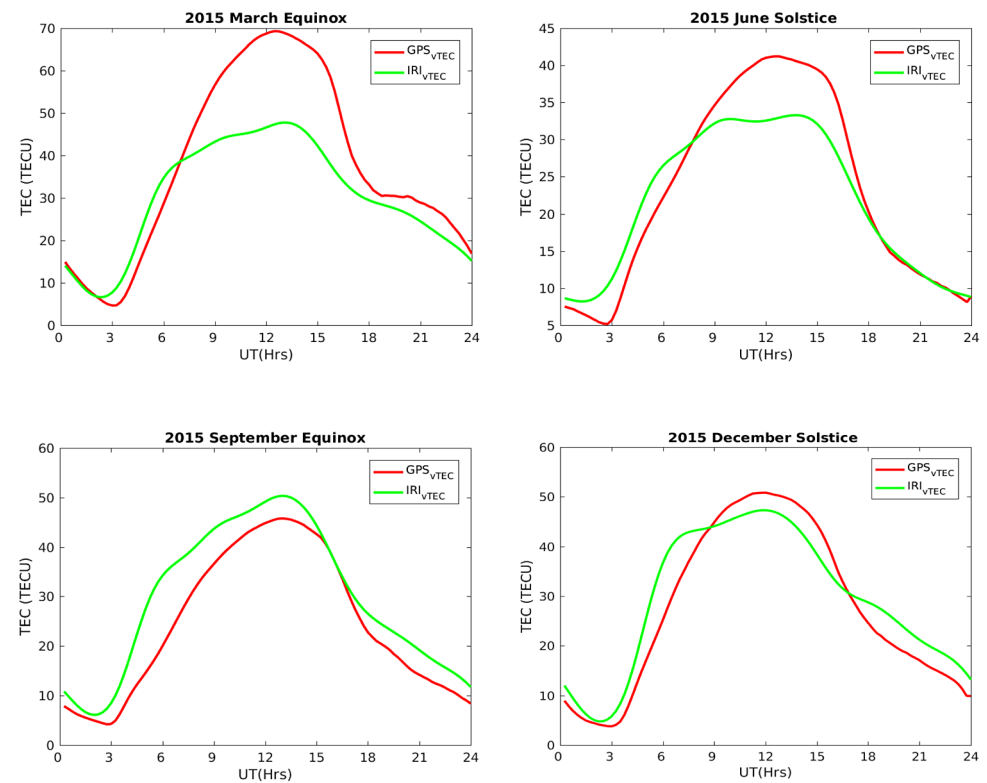
rived GPS-TEC and IRI-TEC demonstrates consistent minimum diurnal, monthly and seasonal mean variations during the presunrise hours 21:00 to 3:00 UT, increases with sharp gradient during the sunrise period (3:00 to 13:00 UT), attains post noon maximum at about 14:00 UT and then falls to a minimum just before sunset. Tariku (2015) studied the

Fig. 14 Seasonal TEC variation and validation of IRI-2016 model and GPS observations in 2016 seasons
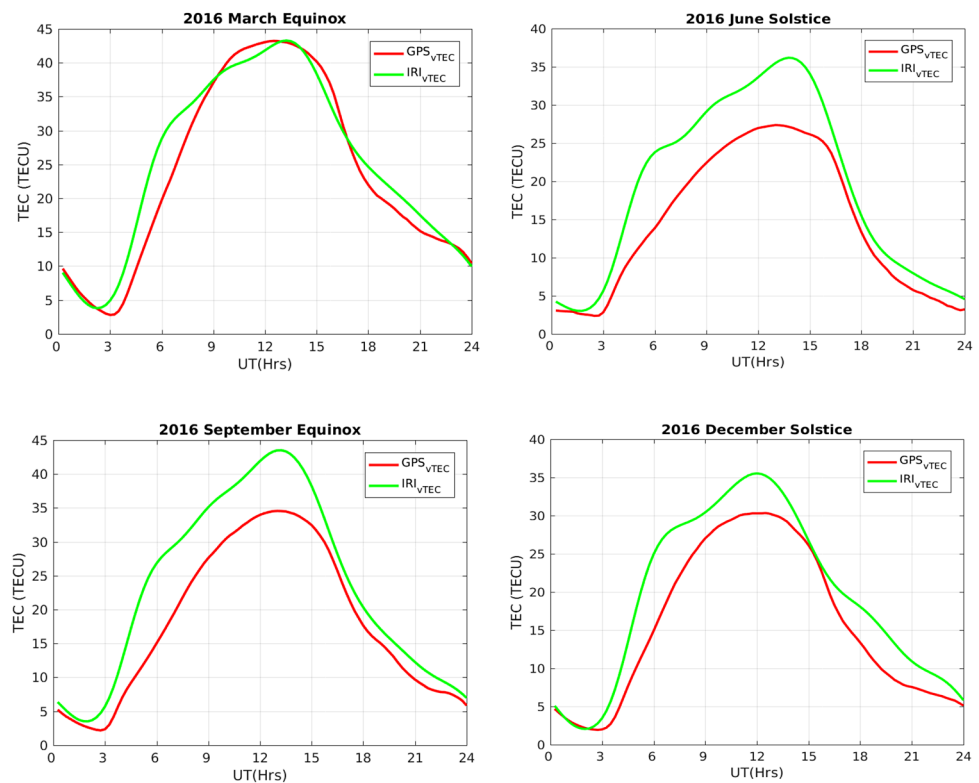
discrepancy in the IRI-2012 model performance using IRI-NeQ topside option over equatorial regions of Ethiopia during low solar activity year 2009 and high solar activity year 2012. His results showed that the diurnal VTEC prediction performance of the model is generally better during the solar minimum phase 2009 than during solar maximum phase 2012 which is in agreement to this study (Tariku et al. 2014). The IRI-2016 model shows slightly small discrepancies in high solar activity phase (2012-2016) by overestimating or underestimating and correlating, which is expected because the IRI model is a model for the ionosphere and does not include the TEC contribution from the plasma sphere. The short coming of this analysis is that the plasmasphere TEC is not taken into account which can be computed using plasmaspheric model (Kumar 2016).

5 Conclusion

In this paper, the patterns of both the measured and modeled TEC variation and capacity of IRI-2016 model in predicting diurnal, monthly, and seasonal TEC variation over Ethiopian region with a focus over Debark station during a high (2012-2016) solar activity phase have been studied. In storm days GPS-VTEC observation values show fluctuations, but the IRI-2016 model VTEC values do not show notable fluctuations in all the five year month days in storm on options. The diurnal, monthly and seasonal maximum TEC occurs in between around 9:00 and 18:00 UT (12:00 and 21:00 LT) hours and the minimum TEC occurs just before and after these hours. The overall results show that IRI-2016 model generally overestimates the diurnal, monthly and seasonal mean VTEC values being observed during the high solar activity (2012-2016) phase. The monthly and seasonal variations of measured VTEC in equinoctial monthly values are higher than in solstice months. The monthly and Seasonal mean of IRI-TEC and GPS-TEC correlates before 9:00 UT/12:00 LT and after 18:00 UT/21:00 LT hours and slightly IRI-TEC underestimates in between these hours.

References

Abdus Salam Intern: Ionospheric Modelling for Theoretical Physics Aeronomy and Radio Propagation Laboratory, Italy (2009)

Akala, A.O., Rabiu, A.B., Somoye, E.O., Oyeyemi, E.O., Adeloye, A.B.: The response of African equatorial GPS-TEC to intense geomagnetic storms during the ascending phase of solar cycle 24. J. Atmos. Sol.-Terr. Phys. **98**, 50–62 (2013)

Athieno: Empirical Model in the Characterization of High Frequency Propagation in the Arctic Region. University of New Brunswick, Fredericton (2017)

Bhuyan, P.K., Borah, R.R.: TEC derived from GPS network in India and comparison with the IRI. Adv. Space Res. **39**(5), 830–840 (2007)

Bilitza, D.: International reference ionosphere: recent developments. Radio Sci. **21**(3), 343–346 (1986)

Bilitza, D.: International reference ionosphere 2000. Radio Sci. **36**(2), 261–275 (2001)

Bilitza, D.: International reference ionosphere 1990, NSSDC/WDC-A-R S 90-22. National Space Science Data Center, Greenbelt (1990)

Bilitza, D., Reinisch, B.W.: IRI-2007: improvements and new parameters. Adv. Space Res. **42**(4), 599–609 (2008)

Bilitza, D., Altadill, D., Zhang, Y., Mertens, C., Truhlik, V., Richards, P., McKinnell, L., Bodo Reinisch, B.: The IRI-2012-A model of international collaboration. J. Space Weather Space Clim. **4**, A07 (2014). https://doi.org/10.1051/swsc/2014004

Bilitza, D., Altadill, D., Truhlik, V., Shubin, V., Galkin, I., Reinisch, B., Huang, X.: International reference ionosphere 2016: from ionospheric climate to real-time weather predictions IRI-2016. Space Weather (2017). https://doi.org/10.1002/2016SW001593

Bittencourt: Fundamentals of Plasma Physics 1, 3rd edn. Springer, New York (2004)

Ciraolo, L., Azpilicueta, F., Brunini, C., Meza, A., Radicella, S.M.: Calibration errors on experimental slant total electron content (TEC) determined with GPS. J. Geod. **81**, 111–120 (2007)

Ezquer, R.G., Jadur, C.A., de Gonzalez, M.M.: IRI-95 TEC predictions for the South American peak of the equatorial anomaly. Adv. Space Res. **22**(6), 811–814 (1998)

Gao, Y., Liu, Z.: Precise ionospheric modelling using regional GPS network data. J. Glob. Position. Syst. **1**(1), 18–24 (2002)

Gonzalez, W., Joselyn, J., Kamide, Y., Kroehl, H., Rostoker, G., Tsurutani, B., Vasyliunas, V.: What is to geomagnetic storm? J. Geophys. Res. **99**, 5771–5792 (1994)

Gopalswamy, N., Yashiro, S., Akiyama, S.: Geoeffectiveness of halo coronal mass ejections. J. Geophys. Res. **112**, A06112 (2007). https://doi.org/10.1029/2006JA012149

Hunsucker, R., Hargreaves, J.: The High-Latitude Ionosphere and Its Effects on Radio Propagation. Cambridge Atmospheric and Space Science Series. Cambridge University Press, Cambridge (2002)

Klobuchar, J.A., Parkinson, B.W., Spilker, J.J.: Ionospheric effects on GPS. In: Global Positioning System: Theory and Applications. American Institute of Aeronautics and Astronautics, Washington (1996)

Kumar, S.: Performance of IRI-2012 model during a deep solar minimum and a maximum year over global equatorial regions. J. Geophys. Res. Space Phys. **121**, 5664–5674 (2016). https://doi.org/10.1002/2015JA022269

Kumar, S., Tan, E.L., Murti, D.S.: Impacts of solar activity on performance of the IRI-2012 model predictions from low to mid latitudes. Earth Planets Space **67**, 42 (2015). https://doi.org/10.1186/s40623-015-0205-3

Limberger, M., Hernandez-Pajares, M., Aragon-Angel, A., Altadill, D., Dettmering, D.: Long-term comparison of the ionospheric F2 layer electron density peak derived from ionosonde data and Formosat-3/COSMIC occultations. J. Space Weather Space Clim. **5**, A21 (2015). https://doi.org/10.1051/swsc/2015023

Liu, L., Chen, Y.: Statistical analysis of solar activity variations of total electron content derived at Jet Propulsion Laboratory from GPS observations. J. Geophys. Res. Space Phys. **114**, A10311 (2009). https://doi.org/10.1029/2009JA014533

Mendillo, M.: Storms in the ionosphere: patterns and processes for total electron content. Rev. Geophys. **44**, RG401 (2006). https://doi.org/10.1029/2005RG000193

Mukherjee, S., Sarkar, S., Purohit, P.K., Gwal, A.K.: Seasonal variation of total electron content at crest of equatorial anomaly station during low solar activity conditions. Adv. Space Res. **46**(3), 291–295 (2010)

Newell, H.E.: Beyond the Atmosphere. NASA SP-4211, Washington, DC (1980)

Nigussie, M., Radicella, S.M., Damtie, B., Nava, B., Yizengaw, E., Groves, K.: Validation of the Ne-Quick and IRI-2007 models in East-African equatorial region. J. Atmos. Sol.-Terr. Phys. (2013). https://doi.org/10.1016/j.jastp.2013.04.016

Olwendo, O.J., Baki, P., Mito, C., Doherty, P.: Comparison of GPS TEC variations with IRI-2007 TEC prediction at equatorial latitudes during a low solar activity (2009-2011) phase over the Kenyan region. Adv. Space Res. **49**, 914–921 (2012a). https://doi.org/10.1016/j.asr.2011.12.007

Olwendo, O.J., Baki, P., Mito, C., Doherty, P.: Characterization of ionospheric GPS total electron content (GPS-TEC) in low latitude zone over the Kenyan region during a very low solar activity phase. J. Atmos. Sol.-Terr. Phys. **84**, 52–61 (2012b). https://doi.org/10.1016/j.jastp.2012.06.003

Oyekola, O.S.: Equatorial vertical plasma drifts and the measured and IRI model-predicted F2-layer parameters above Ouagadougou during solar minimum. Earth Planets Space **64**, 577–593 (2012)

Prolss, G.W.: Physics of the Earth's Space Environment: An Introduction. Springer, Berlin (2004)

Ratcliffe, J.A.: The ionosphere and the engineer. Proc. Inst. Elec. Eng. **114**, 1 (1967)

Rawer, K., Bilitza, D., Ramakrishnan, S.: Goals and status of the International Reference Ionosphere. Rev. Geophys. **16**(2), 177–181 (1978)

Rios, V.H., Medina, C.F., Alvarez, P.: Comparisons between IRI predictions and digisonde measurements at Tucuman. J. Atmos. Sol.-Terr. Phys. **69**, 569–577 (2007)

Sethi, N.K., Dabas, R.S., Sarkar, S.K.: Validation of IRI-2007 against ETC observation during low solar activity over Indian sector. J. Atmos. Terr. Phys. **73**, 751–759 (2011)

Tariku, Y.A.: TEC prediction performance of IRI-2012 model during a very low and a high solar activity phase over equatorial regions, Uganda. J. Geophys. Res. Space Phys. **120**, 5973–5982 (2015). https://doi.org/10.1002/2015JA021203

Tariku, Y.A., Kassa, T., Nigussie, M.: Validation of IRI-2012 TEC model over Ethiopia during solar minimum (2009) and solar maximum (2013). Adv. Space Res. **53**, 1582–1594 (2014). https://doi.org/10.1016/j.asr.2014.02.017

Wernik, A.W., Lucilla, A., Materassi, M.: Ionospheric irregularities, scintillation and its effects on systems. Acta Geophys. Pol. **52**(2), 237–249 (2004)